Journal of the European Ceramic Society 17 (1997) 995–1001

PII: S0955-2219(96)00197-5
0955-2219/97/$17.00

High-Temperature Corrosion of a Silicon-Infiltrated Silicon Carbide Material in Combustion Atmospheres

K. Ghanbari-Ahari & K. S. Coley*

Department of Mechanical Engineering, Metallurgy and Engineering Materials Group, University of Strathclyde, Glasgow G1 1XN, UK

(Received 20 February 1996; revised version received 15 September 1996; accepted 23 September 1996)

Abstract

High-temperature corrosion of a silicon-infiltrated alpha silicon carbide material was investigated, using an atmospheric pressure low-velocity Burner Rig to simulate gas turbine atmospheres with a range of SO_3 partial pressures and sodium concentrations. Experiments were carried out at temperatures above the dew point of sodium sulphate in the range 1250 to 1350°C. Sample weight was monitored for corrosion assessment on a 20 h cyclic basis.

Corrosion followed a parabolic rate law under all conditions studied and the activation energy was found to be 140 kJ mol^{-1}.

It was found that at constant sodium contaminant flux rates P_{SO_3} had a greater effect on corrosion than sodium concentration in the atmosphere. The corrosion rate increased as sulphur trioxide partial pressure decreased. There appeared to be a strong correlation between sodium content of the oxide scale and the rate of corrosion. This is explained by considering oxidation in the presence of sodium to occur by ionic diffusion of oxygen in the glassy scale.

The mechanism of oxidation is discussed, and it is demonstrated that the metallic silicon in the ceramic must oxidise in advance of the silicon carbide in order for the reaction to proceed but it is also shown that the distance separating the two reaction fronts would not be observable in the present circumstances. © 1997 Elsevier Science Limited.

Introduction

Non-oxide silicon-based ceramics (e.g. SiC, Si_3N_4 and Sialons) with superior high-temperature properties are candidates for use in a number of combustion applications[1,2] including gas turbines.[3,4]

The major cause of corrosion in metallic gas turbines is sodium sulphate which deposits on components and reacts with the protective oxide scale reducing its protectiveness.[5,6,7] Corrosion of silicon-based ceramics by molten salt deposits has been studied by a number of workers,[8–12] and has been shown to follow similar principles to the corrosion of alloys. However, there have been relatively few studies on corrosion at temperatures above the dew point of these salts,[11,13–15] which are likely to be representative of the service temperatures of ceramic components. The present study is aimed at assessing the effect of contaminants such as sodium and sulphur at temperatures above the dew point of sodium sulphate, on the corrosion of silicon carbide.

Burner rigs have been found to be the most effective method of simulating gas turbine environments in the laboratory[16] and the parameters affecting their operation are fairly well understood[16,17] when operating below the dew point of sodium sulphate. Therefore a low-velocity burner rig has been employed in the current work to investigate the corrosion of silicon carbide.

Hancock[18] has suggested that sodium contaminant flux rate (CFR) is the critical parameter in controlling corrosion rate and Saunders *et al.*[19] suggested that deposition rate, which is related to CFR, is critical. In the present circumstances, where we are operating above the dew point of sodium sulphate, the critical operating parameters are expected to be somewhat different.[13] The conditions chosen for the present study based on those recommended for a recent VAMAS round robin on testing of superalloys,[20] were varied in order to determine the relative importance of contaminant flux rate, sodium oxide partial pressure, and sulphur trioxide partial pressure. These

*To whom correspondence should be addressed at: Department of Materials Science and Engineering, McMaster University, Hamilton, Ontario L8S 4L7, Canada.

conditions not only have the advantage of being consistent with those employed on metallic materials,[16] but are also identical to conditions employed in a recent study on materials very similar to that in the current investigation.[14]

Experimental Procedure

Alphalite SiC material used in this study was supplied by Kanthal, and is manufactured by slip-casting in the form of rods with a diameter of 6 mm and length of 120 mm. This material consists of 85 wt% α-silicon carbide 15 wt% free silicon and is almost 100% of theoretical density. It is fired at $T<1400$°C and a maximum working temperature of 1300°C is recommended. Figure 1 shows the as-received material, where there is evidence of inhomogeneity in the distribution of silicon. Samples were centreless ground to give a surface roughness parameter of 0·8 to 1·4 μm and nominal dimensions of 5 mm diameter and 55 mm length. Samples were washed with acetone and methanol, then dried overnight in an oven at 250°C; their weights were determined, using a balance, to five decimal places (10 μg).

A low-velocity burner rig, which is heated electrically and capable of giving operating (sample) temperatures of up to 1350°C, was used for corrosion studies of the prepared samples. The burner rig has been described in some detail elsewhere.[21] The combustion atmosphere was simulated by injecting 1·2 cc/min of a low ash content fuel oil (1 wt% sulphur), and 0·8 cc/min diluted synthetic sea water (ASTM D1141 diluted by a factor of 4)[20] into the air stream flowing into the combustion chamber at 25 l/min. The condition achieved by this procedure is given in Table 1 as Condition 1. Additional experiments were carried out, in an attempt to determine critical operating parameters for burner rig testing at temperatures above the dew point of sodium sulphate. During these experiments the flow rates of fuel and air were set to half of those for Condition 1 to create Condition 2 and a further reduction of fuel to zero with the air flow as for Condition 2, resulted in Condition 3. In addition, some experiments were conducted in laboratory air for comparison and this is termed Condition 4 in Table 1. The partial pressures of the gaseous species have been calculated using SOLGASMIX[22] with data obtained from the JANAF Tables[23] and those of critical species are quoted in Table 1.

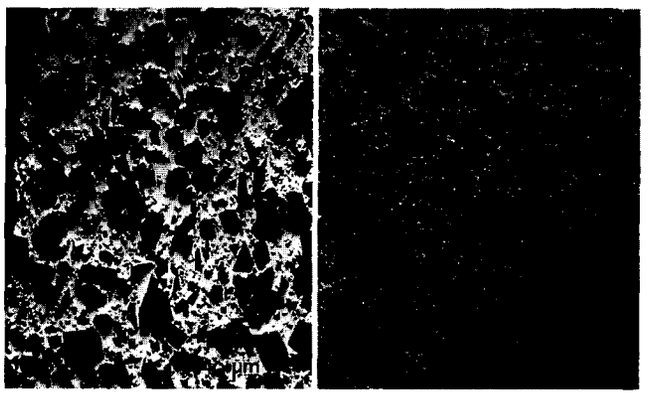

Fig. 1. As-received silicon carbide demonstrating some level of inhomogeneity in silicon metal distribution, (a) centre of sample, (b) surface of sample.

Samples were mounted on a carousel (made from a high-alumina castable refractory) in a vertical position. The carousel was then placed in the combustion chamber of the burner rig, which was already at the experimental temperature, and rotated at 10 rpm in the flowing gas stream. The extent of corrosion was assessed by determining sample weight change at the end of each 20-h cycle. At the end of each cycle, samples were removed from the burner rig at temperature and immediately placed in an insulating chamber to reduce the cooling rate in order to prevent cracking or spalling of the corrosion scale. After cooling to room temperature samples were weighed to an accuracy of 10 μg. Attempts were made to measure section loss but the amount of loss was too low to measure with a reasonable accuracy therefore weight change was used as the measure of corrosion.

Results and Discussion

Visual examination of samples showed that corrosion products form a uniform glassy scale which is shown by EDAX analysis to contain a high level of calcium and sodium picked up from the combustion atmosphere, as shown in Table 2. There was no evidence that the non-uniform silicon distribution in the original material affected the corrosion.

The specific weight gain versus square root of time is shown in Fig. 2 for samples exposed at temperatures 1250, 1300 and 1350°C under Condition 1. Rate constant values are tabulated in Table 3. Oxidation of this material follows a parabolic rate law which suggests that the reaction is controlled predominantly by a diffusion step. However, the parabolic rate curves for 1250 and 1300°C exhibit an 'incubation period'. This could be due to a chemical reaction step being rate-limiting prior to the oxide layer reaching sufficient thickness to control the corrosion rate or to a pre-existing oxide layer which contains no impurities and therefore is less permeable to oxygen. In the latter case the incubation time would be

Table 1. Burner rig operating conditions and parabolic rate constants

Condition	P_{Na_2O} *(atmos* $\times 10^{13}$*)*	P_{SO_3} *(atmos* $\times 10^{6}$*)*	P_{O_2} *(atmos* $\times 10^{13}$*)*	*Na CFR* *(g cm^{-2} h^{-1}* $\times 10^{-3}$*)*	k *(g^{2}cm^{-4}s^{-1}* $\times 10^{12}$*)*
1	1·3	2·3	0·097	3·6	4·3
2	2·8	2·3	0·092	3·6	4·3
3	3·0	0	0·18	3·6	6·0
4	0	0	0·21	0	0·22

the time for the sodium content of the scale to increase to its equilibrium level. The plot for 1350°C does not show this incubation time but this would be consistent with either of the proposed mechanisms. Chemical reaction steps tend to have higher activation energies than diffusion steps and therefore are less likely to be rate-controlling at higher temperatures. If the incubation time is related to the time to reach sodium saturation we would also expect this to be shorter at higher temperatures.

The effect of temperature on the parabolic rate constant is shown in Fig. 3. This silicon-infiltrated SiC material exhibits an activation energy of 104 kJ/mol for corrosion in combustion atmosphere (Condition 1) which is representative of that for molecular diffusion of oxygen in silicate glasses.[24,25]

Samples corroded under different conditions looked very much alike. Specific weight gain values (at T=1300°C) for Conditions 1 and 2 were very similar but removing sulphur from the system, Condition 3, had more effect on the corrosion rate, as shown in Fig. 4.

From these results it appears that changing the sodium oxide activity at a constant contaminant flux rate makes little difference to the corrosion rate, whereas decreasing the sulphur trioxide partial pressure increases the corrosion rate. Analysis of the oxide scale shows little difference in corrosion Conditions 1 and 2 although the calculated sodium oxide activity is a factor of two greater for Condition 2. However the low sulphur trioxide pressure (Condition 3), leads to an increase in sodium oxide content. Although there was some scatter in the analyses of the scale there was no evidence of a gradient in sodium concentration across the scale. The corrosion rate in air, Condition 4, is very much lower than in any of the sodium-bearing atmospheres, Table 1. These results are consistent with the work of other authors[26] and are believed to be due to sodium decreasing the viscosity of the scale thereby increasing the transport rate of oxygen, although this would not be consistent with molecular diffusion as a rate-determining step.[27] These results are also in complete agreement with previous work by the authors on corrosion of silicon nitride,[13] although the magnitude of the effect does not appear to be as great in the present case.

It is clear that the increased sodium contamination in the scale has resulted in faster corrosion rates. However, it is much less clear why there should be an increase in changing conditions from

Table 2. EDX analysis of samples corroded at 1300°C (compositions are expressed as wt% of detectable elements)

Atmosphere *Phase*	*Cond. 1* *Silicon*	*SiC*	*Scale*	*Cond. 3* *Scale*
Si	99·8	98·85	78·98	78·2
Al	—	—	2·74	0·54
Na	0·2	0·06	3·64	6·33
K	—	—	0·71	0·16
Ca	—	—	9·88	14·24
Mg	—	0·24	4·04	0·53
S	—	—	—	—

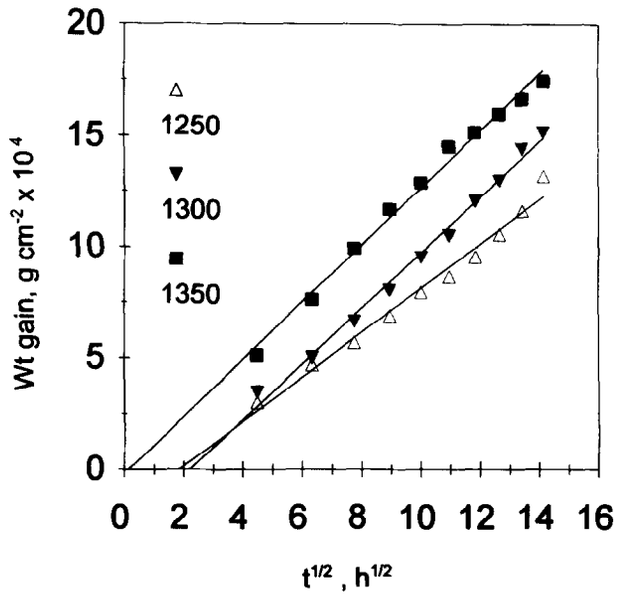

Fig. 2. Parabolic rate plot for samples exposed in the burner rig at 1250, 1300 and 1350°C, Condition 1. Each data point is average of four measurements. The lines have been obtained using linear regression.

Table 3. Parabolic rate constant at different temperatures under Condition 1

Temperature (°C)	k *(g^{2}cm^{-4}s^{-1}* $\times 10^{12}$*)*
1250	2·8
1300	4·3
1350	4·6

1 to 3 and not in changing from Condition 1 to 2. Hancock[18] has suggested that when there is deposition involved CFR is the critical parameter in controlling the rate of burner rig corrosion. However, in the present work, where we are operating above the dew point of sodium sulphate, and would expect conventional gas phase corrosion, the partial pressures of the reactive species should be more important than the flux of these species. From the results of the present work that does not appear to be the case. The effect of SO_3 partial pressure is also more akin to behaviour in the presence of a deposit than would be expected at temperatures above the dew point of sodium sulphate.

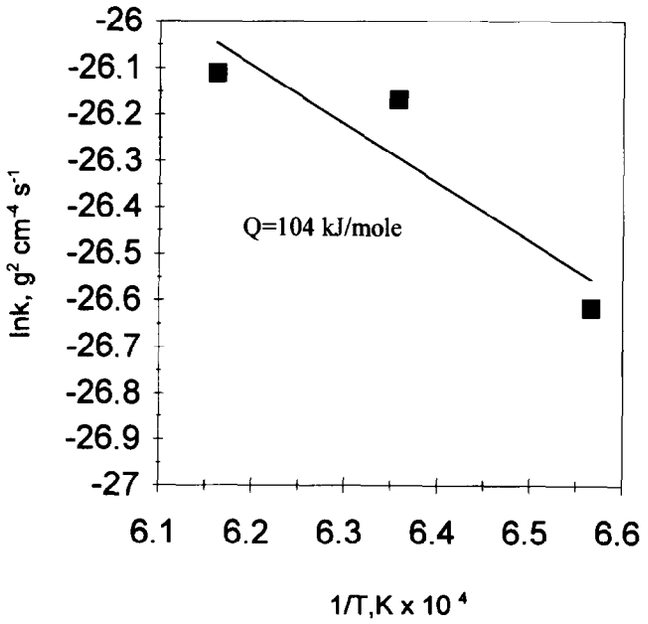

Fig. 3. Temperature dependence of parabolic rate constant for corrosion under Condition 1.

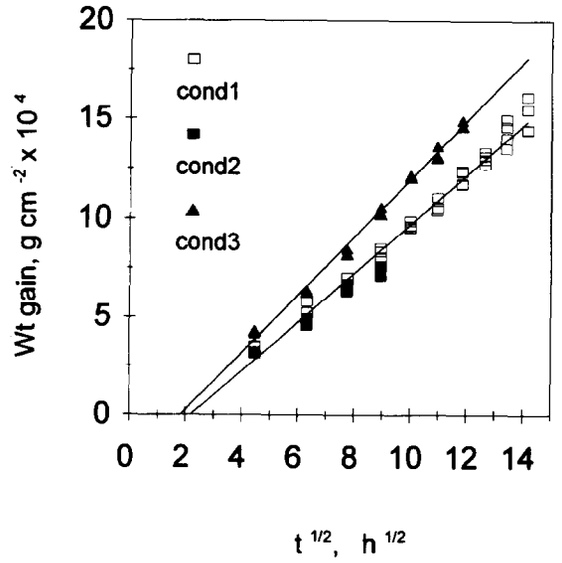

Fig. 4. Comparison of parabolic rate plots for samples exposed in the burner rig at 1300°C under Conditions 1, 2 and 3.

If we consider the reaction

$$Na_2SO_4 = Na_2O + SO_{3(g)}, \quad K = \frac{a_{Na_2O} \cdot P_{SO_3}}{a_{Na_2SO_4}} \quad (1)$$

we can see that at a constant activity of sodium sulphate, $a = 1$ for the case of deposition, the sodium oxide activity will be inversely proportional to P_{SO_3} therefore we will have a high sodium oxide activity at low P_{SO_3}. On the other hand, in this case there can be no deposition of sodium sulphate, and furthermore the major sodium-bearing species in the gas phase are sodium chloride and sodium hydroxide.[23,28] Therefore the sodium oxide activity, which is the driving force for sodium dissolution in the scale, cannot be controlled by eqn (1). In a previous publication[13] the authors suggested that the effect of SO_3 on the rate of corrosion of silicon nitride could be due to SO_3 itself being incorporated in the scale rather than an indirect effect on the activity of Na_2O. However, there is no evidence for sulphur incorporation in the scale and there is clear evidence for a change in sodium oxide content with P_{SO_3}.

The most likely explanation for this inconsistency between calculation and observation is that the thermodynamic data are inaccurate and that sodium sulphate is indeed the predominant gaseous species, in which case eqn (1) would dictate the sodium oxide activity. It is clear that further work is required in order to determine the exact role of contaminants such as sulphur and sodium.

Having accepted that there is some discrepancy between theoretical prediction and experimental behaviour, in relation to the role of sodium oxide activity and sulphur trioxide partial pressure, it is clear that sodium contamination in the scale increases the corrosion rate. This result in itself presents some difficulty because, it is generally accepted that 'silica formers' oxidise by molecular oxygen diffusion[25] and network modifiers such as sodium oxide would be expected to slow molecular diffusion.[27] On the other hand, network modifiers will decrease the viscosity of the glassy scale and increase the rate of ionic diffusion.[29] It is therefore likely that silicon carbide oxidises by molecular diffusion in laboratory air, but in the presence of contaminants ionic diffusion is the primary transport mechanism. This is consistent with the mechanism proposed by Pareek and Shores[26] for oxidation in the presence of potassium.

Mechanism of attack

The parabolic nature of the reaction kinetics indicates that a diffusion process is the dominant rate-determining step although it does not exclude an element of mixed control. If we consider the

possible diffusion steps, we have either the inward diffusion of oxygen, as O_2 molecules or O^{2-} ions, or the outward diffusion of CO.

As a number of workers have proposed that the oxidation of silica formers is controlled by molecular diffusion of oxygen[24,30,31] we will start by considering this to be the rate-determining step. The flux of oxygen which will be directly proportional to the rate of oxidation is given by eqn (2).

$$J_{O_2} = D_{O_2} \cdot S_{O_2} \frac{(P_{O_2} - P^i_{O_2})}{x} \tag{2}$$

Where, D_{O_2} is the diffusivity of molecular oxygen in the scale, S_{O_2} is the molecular solubility of oxygen in the scale, x is the scale thickness, P_{O_2} is the external oxygen partial pressure and $P^i_{O_2}$ is the oxygen partial pressure at the scale/ceramic interface. In the present case our material contains 15% free silicon, therefore the oxygen partial pressure at the scale/ceramic interface will be controlled by the reaction given in eqn (3).

$$Si + O_2 = SiO_2, \quad K_{1573K} = 9.12 \times 10^{20} \tag{3}$$

This gives $P^i_{O_2} = 1{\cdot}1 \times 10^{-21}$ atmosphere. As this is very much less than the external oxygen partial pressure we can consider

$$P_{O_2} - P^i_{O_2} = P_{O_2} = 9{\cdot}7 \times 10^{-2} \text{ atmosphere.}$$

$$J_{O_2} = 9{\cdot}7 \times 10^{-2} \frac{(D_{O_2} \cdot S_{O_2})}{x}$$

In order for oxidation to proceed the outward flux of CO must be two-thirds that of O_2 otherwise there will be a build-up of CO which will inhibit the oxidation of silicon carbide according to eqn (4).

$$SiC + \frac{3}{2}O_2 = SiO_2 + CO, \qquad K_{1573K} = 1{\cdot}63 \times 10^{27} \tag{4}$$

If we assume $P^i_{O_2}$ is in equilibrium with silicon, $P^i_{CO} = 5{\cdot}9 \times 10^{-5}$ then we can calculate the flux of CO from eqn (5) which is analogous to eqn (2).

$$J_{CO} = D_{CO} \cdot S_{CO} \frac{(P_{CO} - P^i_{CO})}{x} \tag{5}$$

We can assume that $P_{CO} = 0$ and that D_{CO} and S_{CO} are very similar to D_{O_2} and S_{O_2} as the molecules are of a similar size. This assumption, that gases of similar molecular size have similar molecular solubilities and diffusivities in glasses, has been shown to be widely applicable.[33] Therefore we would expect J_{CO} to be 10^{-4} times less than J_{O_2}, which would lead to an increase in P_{CO} and the oxidation of SiC would cease, leading to preferential oxidation of silicon metal. Metallographic examination, both optical and SEM, showed no evidence of preferential oxidation of silicon suggesting some deficiency in the foregoing analysis. However, it is instructive at this stage to consider the extent to which silicon oxidation must precede that of silicon carbide. Consider Fig. 5 showing a schematic representation of oxidation of adjacent grains of silicon and silicon carbide. Figure 5(b) shows the oxygen and carbon monoxide partial pressure gradients across the scale that would exist according to the foregoing hypothesis. If silicon is preferentially oxidised ahead of the silicon carbide, eqn (3) will no longer fix the oxygen partial pressure at point B. The pressures of CO and O_2 will be given by simultaneous solution of the following equations:

$$D_{O_2} \cdot S_{O_2} \frac{(P_{O_2} - P^i_{O_2})}{x} = \frac{3}{2} D_{CO} \cdot S_{CO} \frac{P^i_{CO}}{x}$$

and from eqn (4)

$$P^i_{CO} = 1{\cdot}63 \times 10^{27} (P^i_{O_2})^{\frac{3}{2}}$$

as $D_{O_2} \simeq D_{CO}$ and $S_{O_2} \simeq S_{CO}$

$$P_{O_2} - P^i_{O_2} = \frac{3}{2}(1{\cdot}63 \times 10^{27})(P^i_{O_2})^{\frac{3}{2}}$$

as $P_{O_2} - P^i_{O_2} \simeq P_{O_2} = 9{\cdot}7 \times 10^{-2}$, $P^i_{O_2} = 1{\cdot}16 \times 10^{-19}$ then $P^i_{CO} = 6{\cdot}47 \times 10^{-2}$ (i.e. = 2/3 of P_{O_2}).

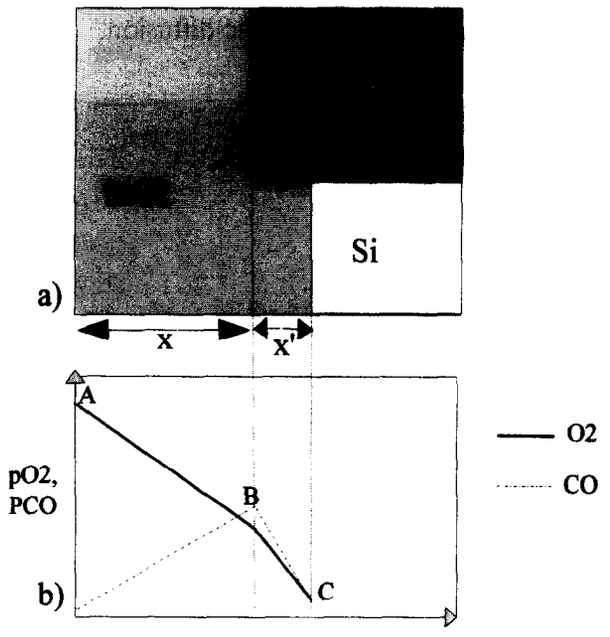

Fig. 5. Schematic representation of oxidation of adjacent grains of silicon and silicon carbide.

The important result from this calculation is the small value for $P^{i}_{O_2}$ which is the driving force for diffusion of oxygen across x'.

$$J'_{O_2} = (1{\cdot}16 \times 10^{-19} - 1{\cdot}11 \times 10^{-21})\frac{D_{O_2} \cdot S_{O_2}}{x'}$$

$$= 1{\cdot}15 \times 10^{-19}\frac{D_{O_2} \cdot S_{O_2}}{x'}$$

J'_{O_2} is the flux of oxygen across x'.

As dp'_{O_2}, the oxygen partial pressure change across x', is about 18 orders of magnitude less than dp_{O_2}, the size of x' will be negligible in relation to x and although for oxidation to proceed the silicon must oxidise in advance of the silicon carbide, the distance between the reaction fronts would not be observable, Fig. 6. No attempt was made to use TEM to assess the difference between the reaction fronts as according to the foregoing analysis there would have been none observable.

The foregoing calculation is an approximation because the oxidation of 15% free silicon was not taken into account when calculating the CO mass balance. However to be more rigorous would make no difference to the argument and negligible difference to the calculated partial pressures (15% change in 18 orders of magnitude).

Having established that the observed reaction kinetics can be explained by diffusion of molecular oxygen as the rate-determining step we are faced with the further complication of the effect of contaminants. In the previous section it was argued that the likely transport process, for oxygen in the presence of sodium, is ionic diffusion. Ionic diffusion of oxygen further complicates analysis of oxidation mechanism as the oxygen flux may not be a linear function of P_{O_2} and it is unlikely that CO product gas can escape by ionic diffusion.

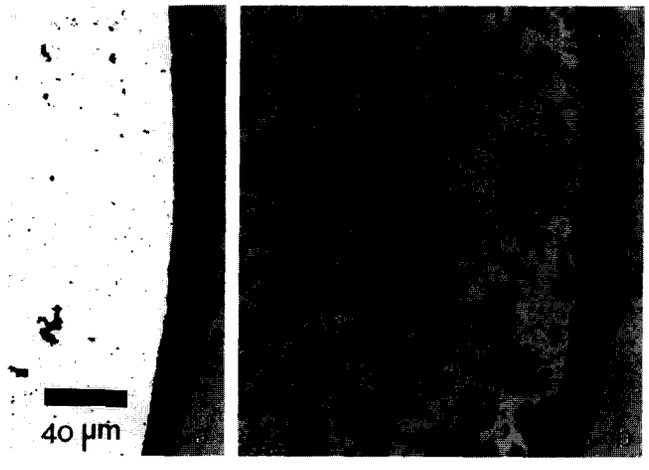

Fig. 6. Photomicrograph demonstrating an oxidised sample at 1300°C for 147 h; (a) and (b) show the same micrograph printed to give different levels of contrast in order to show all salient features. The apparent crack at the interface is an artefact created during printing.

If, in the absence of data to the contrary, we assume that the flux of oxygen is linearly dependent on P_{O_2}, we can describe the oxygen flux by a similar equation to eqn (2) but, as the rate of oxidation in contaminated atmospheres is more than an order of magnitude greater, the product of terms D_{O_2} and S_{O_2} must be more than an order greater. In order to avoid a build-up of CO the flux of CO must also increase by more than an order of magnitude, but as $D_{CO}S_{CO}$ remains the same as for the analysis of molecular diffusion control, P^{i}_{CO} must increase by more than an order of magnitude. In fact, it is likely that $D_{CO}S_{CO}$ will be less in a contaminated scale as it has been shown that molecular permeability normally decreases with increasing concentration of network modifiers.[27,33] but in the absence of data we can only assume that at most the value will be the same as in the uncontaminated case.

Under the present conditions this would raise the CO partial pressure to a level where gas bubble formation may be possible. There is some evidence to support this conclusion in Fig. 6 where a few small bubbles can be seen in the scale. Luthra[32] has suggested that no bubbles will form unless the permeability of oxygen is much greater than that of CO which in this case would be so, as oxygen will diffuse by ionic diffusion in the scale but CO will not.

Conclusion

Alphalite SiC material was corroded at temperatures in the range 1250 to 1350°C in simulated combustion atmospheres with various SO_3 partial pressures.

Oxidation followed a parabolic rate law under all conditions studied and exhibited an activation energy of 104 kJ/mol, which is consistent with molecular oxygen diffusion through silica scales. However sodium contamination was found to enhance the corrosion rate which suggests that ionic diffusion is the predominant transport mechanism.

In the absence of sulphur the corrosion rate increased by a factor of 1.6, which appears to be related to the activity of sodium oxide. Further work is required before a satisfactory explanation can be offered for this result.

At constant contaminant flux rates P_{SO_3} appears to have more effect on the corrosion than sodium concentration in the gas phase but more work is required on the relative importance of these parameters.

The mechanism of corrosion was discussed, and it was demonstrated that for the present conditions,

silicon metal must oxidise in preference to silicon carbide, but the separation of the two reaction fronts would be too small to observe.

Acknowledgements

The authors are indebted to Dr S Pickering of The Centre for Advanced Materials, Petten for supplying the SOLGASMIX computer programme, to Kanthal Ltd for supplying the SiC and to EPSRC for funding the research.

References

1. Jacobson, N. S., Corrosion of silicon-based ceramics in combustion environments. *J. Am. Ceram. Soc.*, 1993, **76**(1), 3–28.
2. Parker, D. A., *Metals and Materials*, 1990, **6**, 14.
3. Callum, G. H. and Smith, T. E., Ceramic composite for aircraft gas turbine engines. *AIAA Paper No. 91-1892.* American Institute of Aeronautics and Astronautics, Washington, DC, June 1991.
4. Bennett, A., Requirements for engineering ceramics in gas turbine engine. *Materials Science and Technology*, 1986, **2**, 895–899.
5. Nishikita, A., Numata, H. and Tsuru, T., *Materials Science and Engineering*, 1991, **A146**, 15.
6. Rapp, R. A., *Materials Science and Engineering*, 1987, **87** 319.
7. Stringer, J., *Materials Science and Technology*, 1987, **3**, 482.
8. Jacobson, N. S. and Fox, D. S., *J. Am. Ceram. Soc.*, 1988, **71**, 139.
9. Mayer, M. I. and Riley, F. L., *J. Material Science*, 1978, **13**, 1319.
10. Jacobson, N. S., Stearns, C. A. and Smialek, J. L., *Adv. Ceram. Mater.*, 1986, **1**, 145.
11. Jacobson, N. S. and Smialek, J. L., *J. Am. Ceram. Soc.*, 1985, **68**(8), 432–439.
12. Smialek, J. L. and Jacobson, N. S., *J. Am. Ceram. Soc.*, 1986, **69**(10), 741–752.
13. G-Ahari, K., Coley, K. S., Baxter, D. J. and Hendry, A., In *Advances in Science and Technology 9: High Temperature Materials in Engine Technology*, ed. P. Vicinzini. Techna Publications, 1995, p. 411.
14. Graziani, T., Baxter, D. J. and Nannetti, C. A., *Key Engineering Materials*, 1996, **113**, 153–164.
15. Booth, G. C. and Clarke, R. L., *Materials Science and Technology*, 1986, **2**, 272.
16. Saunders, S. R. J. and Nicholls, J. R., Hot salt corrosion testing — An international intercomparison. *Materials at High Temperatures* (in press).
17. Nicholls, J. R. and Saunders, S. R. J., Comparison of hot-salt corrosion behaviour of superalloys in high and low velocity burner rigs. *High Temperature Technology*, 1989, **7**, 193–201.
18. Hancock, P., *Corros. Sci.*, 1982, **22**, 51.
19. Saunders, S. R. J., Hossain, M. K. and Ferguson, J. M., In *High Temperature Alloys for Gas Turbines*, ed. R. Brunetaud *et al.* D. Reider Publishing Co., Dordrecht, 1982, 177.
20. Saunders, S. R. J. and Nicholls, J. R., The need for a standard procedure in hot-salt corrosion testing. Guidelines for hot-salt corrosion burner rig tests. *High Temperature Technology*, 1989, **7**, 232–240.
21. G-Ahari, K., Coley, K. S. and Nicholls, J. R., Statistical evaluation of corrosion of sialon in burner rig simulated combustion atmospheres. *J. Eur. Ceram. Soc.*, (submitted).
22. Erikson, G., *Chemica Scripta*, 1975, **8**, 10.
23. Stull, D. R. and Prophet, H., *JANAF Thermochemical Tables, NSRDS-NBS37.* US Dept Commerce, Washington, DC, 1971.
24. Lamkin, M. A., Riley, F. L. and Fordham, R. J., *J. Eur. Ceram. Soc.*, 1992, **10**, 347.
25. Atkinson, A., *Reviews of Modern Physics*, 1995, **57**, 437–470.
26. Pareek, V. and Shores, D. A., *J. Am. Ceram. Soc.*, 1991, **69**, 556.
27. Shelby, J. E., Molecular Solubility and Diffusion. In *Glass II, Treatise on Materials Science and Technology*, Vol. 17, ed. M. Tomozama and R. H. Doremus. Academic Press, New York, pp. 1–40.
28. Kohl, F. J. Stearns, C. A. and Fryburg, G. C., The role of NaCl in flame chemistry, in the deposition process and in its reactions with protective oxides. In *4th UK/US Conference on Gas Turbine Materials in a Marine Environment*, Annapolis, June 1979. US Naval Sea Systems Command, Washington, DC, pp. 565–590.
29. Frischat, G. H., *Ionic Diffusion in Oxide Glasses.* Trans Tech Publ, Bay Village, Ohio, 1975.
30. Zheng, Z., Tressler, R. E. and Spear, K. E., Oxidation of single crystal silicon carbide. *J. Electrochem. Soc.*, 1990, **137**, 850–855.
31. Singhal, S. C., *J. Materials Science*, 1976, **11**, 500.
32. Luthra, K. L., Some new perspectives on oxidation of silicon carbide and silicon nitride. *J. Am. Ceram. Soc.*, 1991, **74**(5), 1095–1103.
33. Doremus, R. H., *Glass Science.* Wiley, New York, 1973.